EPJ manuscript No.
(will be inserted by the editor)

Photo-response of the $N = Z$ nucleus ^{24}Mg

J. Deary[1,2], M. Scheck[1,2a], R. Schwengner[3], D. O'Donnell[1,2], D. Bemmerer[3], R. Beyer[3], Th. Hensel[3,4], A. R. Junghans[3], T. Kögler[3], S. E. Müller[3], K. Römer[3], K. Schmidt[3], S. Turkat[3], S. Urlaß[3], A. Wagner[3], M. Bowry[1,2], P. Adsley[5,6], O. Agar[1,2,7], R. Chapman[1,2], F. C. L. Crespi[8,9], D. T. Doherty[10], U. Friman Gayer[11,12], R.-D. Herzberg[13], J. Isaak[14], R. V. F. Janssens[11,12], T. Kröll[14], B. Löher[15], B. S. Nara Singh[1,2], P. von Neumann-Cosel[14], L. Pellegri[5,6], E. E. Peters[16], G. Rainovski[17], D. Savran[15], J. F. Smith[1,2], M. Spieker[18], P. G. Thirolf[19], S. Triambak[20], W. Tornow[11,21], M. Venhart[22], M. Wiedeking[5,6], O. Wieland[8], S. W. Yates[16], and A. Zilges[23]

[1] School of Computing, Engineering, and Physical Sciences, University of the West of Scotland, Paisley, PA1 2BE, UK
[2] SUPA, Scottish Universities Physics Alliance, UK
[3] Helmholtz-Zentrum Dresden-Rossendorf, 01328 Dresden, Germany
[4] Technische Universität Dresden, Institut für Kern- und Teilchenphysik, 01062 Dresden, Germany
[5] School of Physics, University of the Witwatersrand, Johannesburg 2050, South Africa
[6] iThemba Laboratory for Accelerator Based Sciences, Somerset West 7129, South Africa
[7] Department of Physics, Karamanoglu Mehmetbey University, Karaman, Turkey
[8] INFN, Sezione di Milano, I-20133 Milano, Italy
[9] Department of Physics, Milano University, Milano, 2-133, Italy
[10] Department of Physics, University of Surrey, Guildford, GU2 7XH, UK
[11] Triangle Universities Nuclear Laboratory, Durham, NC 27708-0308, USA
[12] Department of Physics and Astronomy, University of North Carolina at Chapel Hill, Chapel Hill, NC 27599, USA
[13] Department of Physics, Oliver Lodge Laboratory, University of Liverpool, Liverpool L69 7ZE, UK
[14] Institut für Kernphysik, Technische Universität Darmstadt, D-64289 Darmstadt, Germany
[15] GSI Helmholtzzentrum für Schwerionenforschung GmbH, D-64291 Darmstadt, Germany
[16] Departments of Chemistry and Physics & Astronomy, University of Kentucky, Lexington, KY, 40506-0055, USA
[17] Faculty of Physics, St. Kliment Ohridski University of Sofia, 1164 Sofia, Bulgaria
[18] Department of Physics, Florida State University, Tallahassee FL 32306, USA
[19] Ludwig–Maximilians–Universität München, D-85748 Garching, Germany
[20] Department of Physics and Astronomy, University of the Western Cape, Bellville 7535, South Africa
[21] Department of Physics, Duke University, Durham, NC 27708-0308, USA
[22] Institute of Physics, Slovak Academy of Sciences, 84511 Bratislava, Slovakia
[23] Institut für Kernphysik, Universität zu Köln, 50937 Köln, Germany

Received: date / Revised version: date

Abstract The electric $E1$ and magnetic $M1$ dipole responses of the $N = Z$ nucleus ^{24}Mg were investigated in an inelastic photon scattering experiment. The 13.0 MeV electrons, which were used to produce the unpolarised bremsstrahlung in the entrance channel of the $^{24}\mathrm{Mg}(\gamma,\gamma')$ reaction, were delivered by the ELBE accelerator of the Helmholtz-Zentrum Dresden-Rossendorf. The collimated bremsstrahlung photons excited one $J^\pi = 1^-$, four $J^\pi = 1^+$, and six $J^\pi = 2^+$ states in ^{24}Mg. De-excitation γ rays were detected using the four high-purity germanium detectors of the γELBE setup, which is dedicated to nuclear resonance fluorescence experiments. In the energy region up to 13.0 MeV a total $B(M1)\uparrow = 2.7(3)\ \mu_N^2$ is observed, but this $N = Z$ nucleus exhibits only marginal $E1$ strength of less than $\sum B(E1)\uparrow \leq 0.61 \times 10^{-3}\ \mathrm{e^2fm^2}$. The $B(\Pi 1, 1_i^\pi \to 2_1^+)/B(\Pi 1, 1_i^\pi \to 0_{gs}^+)$ branching ratios in combination with the expected results from the Alaga rules demonstrate that K is a good approximative quantum number for ^{24}Mg. The use of the known $\rho^2(E0, 0_2^+ \to 0_{gs}^+)$ strength and the measured $B(M1, 1^+ \to 0_2^+)/B(M1, 1^+ \to 0_{gs}^+)$ branching ratio of the 10.712 MeV 1^+ level allows, in a two-state mixing model, an extraction of the difference $\Delta\beta_2^2$ between the prolate ground-state structure and shape-coexisting superdeformed structure built upon the 6432-keV 0_2^+ level.

PACS. 2 0.21.10.Ky, 20.21.10.Pc, 20.21.10.Tg, 20.25.20.Dc, 20.27.30.+t

1 Introduction

Because they can act as doorway states in particle-capture reactions, the structure of low-spin states in light nuclei are of interest in modeling the burning cycles of massive stars in in their final days [1,2]. Particularly interesting are natural parity states for (α,γ) capture reactions of the spin-less α particle and in (p,γ) proton-capture reactions. For the latter reaction the capture states with $J = J_0 \pm 1/2$, where J_0 ground-state angular momentum of the capturing odd-mass nucleus and the $1/2$ represents the spin of the proton, are favored. If such levels are situated just above the respective threshold for α-particle or proton evaporation, a substantial enhancement of the radiative capture rate can be expected. In this energy region the convolution of the capture cross section and the Maxwell-Boltzmann-shaped particle-energy distribution opens the Gamow window for sizeable reaction rates.

As evidenced by its enhanced natural abundance, ^{24}Mg is an important stepping stone in the burning processes of heavier stars. For this nucleus the evaporation thresholds are $Q_\alpha = 9316.55(1)$ keV for α particles, $S_p = 11692.69(1)$ keV for protons, and $S_n = 16531.6(7)$ keV for neutrons [3]. Hence, the 0^+, 1^-, and 2^+ natural parity levels above Q_α will influence the (α,γ) capture rates. Given the ground-state spin of $J_0^\pi = 3/2^+$ [4], the s-wave capture of the ^{23}Na(p,γ) and ^{23}Na(p,α) reactions will be strongly influenced by 1^+ and 2^+ states. Of course, one condition for these levels to be a doorway for a particle-capture reaction is a γ-ray branch to a lower-lying particle-bound state that stabilises the final nucleus against subsequent particle emission. For the inverse reaction of photodissociation, the energies of photo-excitable levels, especially $J = 1$ states, their ground-state excitation width and particle-decay branching ratio are important.

An experimental tool, which can be used to obtain detailed spectroscopic information for low-spin states is the scattering of real photons, the so-called nuclear resonance fluorescence (NRF) process [5,6]. Due to the low momentum of photons, this reaction limits the angular momentum transfer to a good degree to 1 $\hbar$ of the photon intrinsic angular momentum and, less probable, one further unit. Hence, for even-even nuclei this technique is perfectly suited to investigate levels with $J^\pi = 1^-, 1^+$, and 2^+. Indeed, a previous ^{24}Mg(γ,γ') experiment [7] has shown the existence of strongly excited 1^+ states at excitation energies of 9827(3) keV, 9967.5(10), and 10713.0(7) keV. However, due to its focus on $M1$-strength in sd-shell nuclei, no data for 1^- levels and possibly excited 2^+ states is presented in Ref. [7]. It is the intention of this work to provide this additional information.

From a nuclear structure point of view, the $E1$ strength to $J^\pi = 1^-$ levels below the Isovector Giant Dipole Resonance [8,9] is of interest as several mechanisms are proposed to generate the necessary division of center-of-charge and center-of-mass. Clearly, the underlying shell structure plays a role; for sd-shell nuclei, for which no intruder shell can contribute the opposite parity, one-particle one-hole cross-oscillator shell excitations are necessarily involved in a negative-parity excitation. Hence, the number of microscopic configurations is comparably low and the emergence of collective structures such as an eventual toroidal mode can be studied (see Ref. [10] and references therein). The latter argument assumes that for $N = Z$ nuclei the neutron-skin mode of the Pygmy Dipole Resonance [11, 12] is excluded.

A prolate deformed structure is assigned to the ground state of ^{24}Mg (e.g., see Refs. [10,13] and references therein). While the $E_{4_1^+}/E_{2_1^+} = 3.01$ ratio would appear to support rotational character, it is still significantly different from the rotational value of 3.33. However, there is evidence that, due to mixing with the 6432-keV 0_2^+ state the 0_{gs}^+ level is shifted to lower energy, and, consequently, the $E_{4_1^+}/E_{2_1^+}$ ratio is affected. Nevertheless, the present static deformation implies that the projection K of the angular momentum J on the body-intrisic symmetry axis is a good quantum number and, consequently, the Alaga rules [14] are valid. For the decay of an initial state $|J_iK_i\rangle$ to the two final states $|J_{f1}K_{f1}\rangle$ and $|J_{f2}K_{f2}\rangle$, which must be members of the same rotational band, the Alaga rules define a branching ratio R_{Al}:

$$R_{Al} = \frac{B(\Pi L, J_i \to J_{f1})}{B(\Pi L, J_i \to J_{f2})} = \frac{|\langle J_iK_i\Delta J\Delta K|J_{f1}K_{f1}\rangle|^2}{|\langle J_iK_i\Delta J\Delta K|J_{f2}K_{f2}\rangle|^2}. \quad (1)$$

In the specific case of a $J = 1$ level, which is connected via dipole transitions to the final levels $J_{f1} = 2^+$ and $J_{f2} = 0^+$, which are members of a $K = 0$ ground-state band, R_{Al} is

$$R_{Al} = \frac{|\langle 1K_i1\Delta K|20\rangle|^2}{|\langle 1K_i1\Delta K|00\rangle|^2} = \begin{cases} 2 & \text{for } K_i = 0 \\ 0.5 & \text{for } K_i = 1 \end{cases}. \quad (2)$$

Indeed, for well-deformed nuclei in the rare-earth region, NRF experiments have shown that for the majority of $J = 1$ states R_{Al} is distributed around the expected values (e.g., see Ref. [15]).

Furthermore, in ^{24}Mg shape coexistence [16] between the prolate ground-state band and a super-deformed band built on the first excited 0_2^+ level at 6432 keV has been proposed [13]. Using the approach as outlined in Ref. [17], the $R_0 = B(M1, 1_i^+ \to 0_2^+)/B(M1, 1_i^+ \to 0_{gs}^+)$ branching ratio of a 1^+ level to the two shape-coexisting 0^+ levels can be exploited to extract the mixing coefficients. Together with the difference in the square of the deformation parameter $\Delta\beta_2^2$, these coefficients determine the $\rho^2(E0)$ strength (e.g., see Eq. (45) in Ref. [13]). Hence, the known $\rho^2(E0, 0_2^+ \to 0_{gs}^+) \times 10^3 = 380(70)$ value [18] and the measured R_0 branching ratio permit a model-dependent extraction of $\Delta\beta_2^2$.

2 Experiment

The experiment was conducted at the ELBE accelerator of the Helmholtz-Zentrum Dresden-Rossendorf and used the

[a] *email address: marcus.scheck@uws.ac.uk*

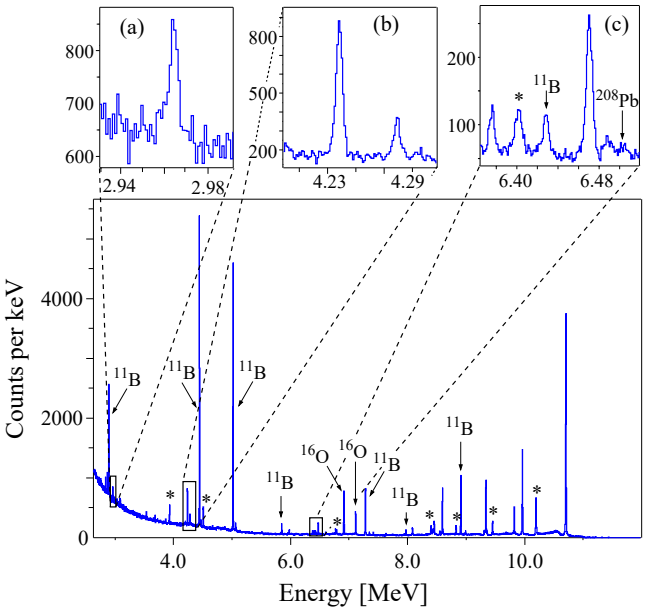

Figure 1. Spectrum resulting from the addition of the spectra recorded in the detectors at $\theta = 127°$. ^{11}B marked peaks belong to transitions of the photon-flux calibration standard boron-11, ^{16}O marks transitions of oxygen-16, and asterisks indicate single- and double-escape peaks. The enlarged parts (a), (b), and (c) of the γ-ray spectrum include low-intensity peaks of newly observed γ rays.

γELBE setup [19] for photon detection. The bremsstrahlung photons in the entrance channel were produced by bombarding a thin niobium radiator target with a beam of 13.0 MeV electrons. Typical beam currents were 425 μA over an accumulated total beam time of approximately 126 hours.

The bremsstrahlung photons enter the γELBE cave via a circular hole in a 2.6 m thick collimator made of aluminium. The γELBE setup consists of four high-purity germanium detectors (HPGe), with two detectors positioned at $\theta = 90°$ and two detectors placed at $\theta = 127°$ with respect to the momentum direction of the photon beam. All detectors have a γ-ray detection efficiency of approximately 100 % relative to the $3'' \times 3''$ NaI calibration standard. Each detector was equipped with an active anti-Compton shield. The target to detector distance was approximately 28 cm for the 90° detectors and 32 cm for the 127° detectors. Each 90° detector covers an angular range of $\Delta\theta = 16°$ and the 127° detectors an interval of $\Delta\theta = 14°$. In order to keep the detector counting rate at ≈10 kHz and reduce the probability of pile-up events, low-energy γ- and X-ray radiation was suppressed by attenuators between target and detector. For the two 90° detectors, the attenuators had thicknesses of 8 mm of natural Pb and 3 mm of Cu, while for the 127° detectors the attenuators consisted of 3 mm of Pb and 3 mm of Cu. The relative γ-ray detection efficiency was simulated using the GEANT software package [20]. A spectrum, created by adding the two spectra recorded in the detectors positioned at $\theta = 127°$, is shown in Fig. 1.

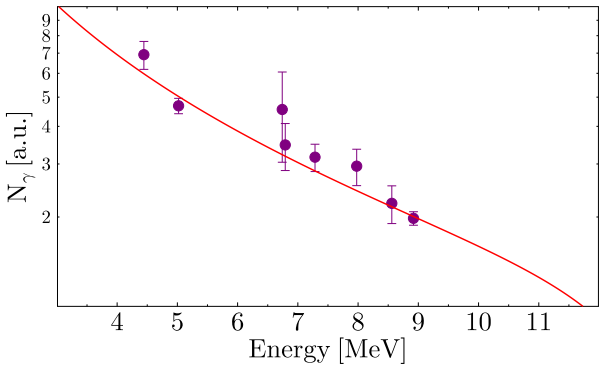

Figure 2. Photon-flux distribution $N_\gamma(E_\gamma)$ represented by the Schiff formula, which is error-weighted fitted to the experimental points of the well-known transitions of ^{11}B. Note the logarithmic scale on the y axis.

In order to minimize absorption effects of the γ rays within the target, it was rotated relative to the incoming photon beam and the front planes of the detectors. The target was made of two discs each of 20 mm diameter. One disc consisted of 3261.1(5) mg of magnesium oxide (MgO). The magnesium was enriched to 99.84 % in the $A = 24$ isotope . The other disc was made of 300.0(5) mg of enriched (99.5 %) ^{11}B. The well-known transitions from photo-excited levels of ^{11}B [21,22,23,25] serve as a photon-flux monitor. This target allows a relative measurement to be made and removes the need to determine absolute γ-ray detection efficiencies $\epsilon_{abs}(E_\gamma)$ and an absolute photon flux $N_{\gamma,abs}(E_L)$. The photon-flux distribution for a thin radiator target is described by the Schiff-formula. An error-weighted fit of this distribution to the experimental points of levels of ^{11}B is shown in Fig. 2. Typical uncertainties in fit of the photon flux were ≈ 2 %; However, to account for systematic effects, such as an extended radiator target or uncertainties with the photon-beam end point, a systemtic uncertainty was added. Within the energy range covered by the photo-excited levels of ^{11}B (4444 keV - 8920 keV) a relative uncertainty of 5 % and outside this range 10 % were assumed for the photon flux.

The energy-integrated scattering cross section, $I_{S,f}$, for a γ-ray transition to the final level, f, is related to experimental quantities

$$I_{S,f} \propto \frac{1}{n_T} \frac{A}{\epsilon(E_\gamma) \cdot N_\gamma(E_L) \cdot W(\theta)}, \qquad (3)$$

namely, the number of target nuclei n_T, the peak area A, the angular distribution function $W(\theta)$, the relative γ-ray detection efficiency $\epsilon(E_\gamma)$, and the relative photon flux $N_\gamma(E_L)$ at the energy of the photo-excited level E_L. Henceforth, energy integrated will indicate that the cross section is integrated over the energy range of the resonance with total decay width $\Gamma = \sum_f \Gamma_f$, corresponding to the sum over the partial decay widths Γ_f for the f decay channels. The relationship between $I_{S,f}$ and the resonance widths is given as

Table 1. Calculated angular distribution functions $W(\theta)$ for the cascade $J_1^\pi \rightarrow J_2^\pi \rightarrow J_3^\pi$. The angle intervals are $W(90°) : 82° - 98°$ and $W(127°) : 120° - 134°$. If a cascade allows a mixed transition multipolarity, the 'pure' multipolarities $\Pi L_{1\rightarrow2}$ and $\Pi L_{2\rightarrow3}$ are indicated. Finally, the expected ratio $R = W(90°)/W(127°)$ is given.

J_1-J_2-J_3	$\Pi L_{1\rightarrow2}$-$\Pi L_{2\rightarrow3}$	$W(90°)$	$W(127°)$	R
0-1-0	$\Pi1$-$\Pi1$	0.755	1.022	0.74
0-2-0	$E2$-$E2$	1.226	0.570	2.15
0-1-1	$\Pi1$-$\Pi1$	1.123	0.989	1.14
0-1-1	$M1$-$E2$	1.123	0.989	1.14
0-1-2	$\Pi1$-$\Pi1$	0.975	1.002	0.97
0-1-2	$M1$-$E2$	0.877	1.001	0.88
0-2-2	$E2$-$M1$	0.877	1.001	0.88
0-2-2	$E2$-$E2$	1.152	0.869	1.33
0-2-3	$E2$-$M1$	1.035	0.997	1.04
0-2-3	$E2$-$E2$	1.071	1.022	1.05

$$I_{S,f} = \pi^2 \left(\frac{\hbar c}{E_L}\right)^2 g\Gamma_0 \frac{\Gamma_f}{\Gamma}, \tag{4}$$

where E_L is the level energy, $g = (2J_L + 1)/(2J_0 + 1)$ a statistical factor, Γ_0 the ground-state width of the excitation path, and Γ_f/Γ the branching ratio of the partial decay width Γ_f and total decay width Γ for the decay path. Considering that the partial decay width $\Gamma_f \propto I_{S,f}$ scales with the energy-integrated scattering cross section and the relation $\tau = \hbar/\Gamma$, the level lifetime τ can be obtained and, subsequently, the reduced transition probabilities $B(\Pi L, J_i \rightarrow J_f)$ determined.

In this work, for a peak to be recognised as such, the following sensitivity limits were applied. If the average background exceeded 20 counts per channel, a Gaussian background distribution was assumed, and it was demanded that the peak area is larger than three standard deviations of the underlying background. If the average background was less than 20 counts per channel, a Poisson distributed background was assumed and a minimum peak area of five standard deviations required.

As mentioned above, in NRF experiments involving an even-even nucleus, states with the angular momentum and parity quantum numbers $J^\pi = 1^\pm$ and $J^\pi = 2^+$ can be populated starting from a 0^+ ground state. In a $0^+ \rightarrow J^\pi \rightarrow 0^+$ cascade. The ratio of the possible angular distribution functions $W(\theta)$ differs most for the angles $\theta_1 = 90°$ and $\theta_2 = 127°$; hence, the detectors were positioned at those angles. This measurement permits an assignment to be made or, if known, confirmation of the level spin. The theoretically calculated values $W(\theta)$ for the detector angular acceptance $\Delta\theta$ are presented for several possible cascades in Table 1. In addition, the calculated $W(90°)/W(127°)$ ratios are presented.

Concerning the assignment of the K quantum numbers via the Alaga rules [14], the value $R_{Al,exp}$ can be related to experimental quantities. Starting from a level J_i to two final levels J_{f1} and J_{f2} of the same rotational band $R_{Al,exp}$ is calculated as

$$R_{Al} = \frac{\Gamma_{f1}}{\Gamma_{f2}} \cdot \frac{E_{\gamma,f2}^{2L+1}}{E_{\gamma,f1}^{2L+1}}, \tag{5}$$

where, $\Gamma_{fi} (i = 1, 2)$ is the decay width for the decay channel fi, $E_{\gamma,fi}$ is the γ-ray energy for the decay channel fi, and L represents the transition multipolarity. If the initial level is a state with $J_i = 1$, the transition must be a dipole $\Pi L = \Pi1$ to the two final levels with $J_{f1} = 2^+$ and $J_{f2} = 0^+$ of the ground-state rotational band. However, in the determination of a decay width via the total decay width $\Gamma = \sum_n \Gamma_n$, the additional uncertainty of the other γ-ray transition enters. In the ratio of the Alaga rules, the total decay width cancels. Furthermore, for two arbitrary decay channels k and l from the same level, the ratio $\Gamma_k/\Gamma_l = I_{S,k}/I_{S,l}$ of partial decay widths Γ_f equals the ratio of the energy-integrated scattering cross sections $I_{S,f}$. Hence, for the practical determination of the branching ratio R_{Al}

$$R_{Al} = \frac{I_{S,f1}}{I_{S,f2}} \cdot \frac{E_{\gamma,f2}^{2L+1}}{E_{\gamma,f1}^{2L+1}} \tag{6}$$

the use of the integrated scattering cross sections $I_{S,fi}$ results in more accurate values. If R_{Al} matches the values given Eq. 2, a K quantum number can be assigned. Any eventual deviation from these optimal branching ratios indicates either K mixing or a deviation from the condition of the validity of the Alaga rules, which means the consideration of the nucleus as a well-deformed rotor.

3 Results

The excellent background conditions at the γELBE setup allowed the identification of many transitions. Besides the desired transitions from ^{24}Mg, transitions associated with the photon-flux calibration standard ^{11}B were identified as well as ^{16}O. Furthermore, the spectra recorded in the detectors at $\theta = 127°$ contained several low-intensity peaks that could be identified as belonging to ^{208}Pb [24]. These γ rays originate from the ^{208}Pb(γ,γ') reaction with the scattered beam in the shielding of the beam dump. While the 90° detectors were actively shielded in this direction, the anti-Compton shield of the 127° detectors has necessarily an opening at these angles. Hence, these γ rays are solely observed in the 127° detectors or exhibit a vanishing $W(90°)/W(127°)$ ratio. Interestingly, a transition at 11442 keV [$W(90°)/W(127°) = 0.31(12)$] was identified from the 11450-keV level in ^{208}Pb [24]. Furthermore, despite the fact that no level in ^{208}Pb is known near the

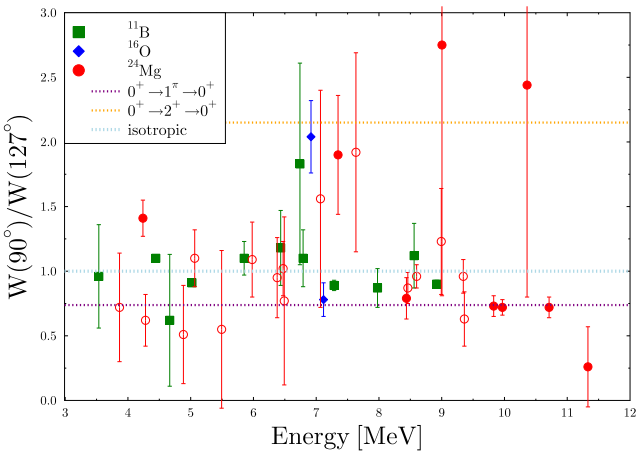

Figure 3. Ratio $W(90°)/W(127°)$ of the angular distribution function at the two angles 90° and 127°, where the detectors were positioned. In addition to the transitions attributed to ^{24}Mg, ratios of transitions from ^{11}B and ^{16}O are shown. Full circles indicate transitions which connect a level in ^{24}Mg to the ground state and open circles represent transitions that end in a lower-lying excited state.

position of a transition at 11324 keV, due to the ratio $W(90°)/W(127°) = 0.27(31)$, it is very likely attributed to depopulate a level in ^{208}Pb near 11330 keV.

The $W(90°)/W(127°)$ ratio for each observed γ ray is presented in Table 2 and is shown, together with values for transitions of ^{11}B and ^{16}O, in Fig. 3. The γ rays are presented together with the energies of the levels they have been assigned to. Additionally, the level spin from the literature [3] is given. The presented γ-ray energies are corrected for recoil effects associated with the momentum transfer in the absorption as well as emission processes. For all of the stronger excited levels of these two reference isotopes, good agreement with the expected values is achieved. For ^{24}Mg, the level spins as found in the literature are confirmed. In principle, for transitions to lower-lying excited states that are possibly of mixed multipolarity, the $W(90°)/W(127°)$ ratio can be used to determine multipole-mixing ratios. However, for NRF the relative uncertainties, which usually exceed 10 %, prevent such a measurement, at least within a meaningful range for the multipole-mixing ratio δ. Nevertheless, in the last column of Table 2, the more likely combination of transition multipolarities is indicated; the angular distribution values associated with this combination were used to calculate the energy-integrated scattering cross section $I_{S,f}$ (see Eq. 3).

Table 3 contains for each transition the extracted energy-integrated scattering cross section $I_{S,f}$, calculated decay width Γ_f, and reduced transition probability $B(\Pi L)\downarrow$.

For several levels, feeding transitions from higher-lying levels are observed. Basically, there are two scenarios. First, the level was exclusively populated by feeding and, consequently, in Table 3, no $I_{s,f}$ and subsequent quantities are given. Second, if a level was populated by photon scattering from the ground state as well as feeding, the $I_{S,f}$ is given as an upper limit, which is here the sum of the calculated value plus the uncertainty. The set of measured $I_{S,f}$ values was used to calculate the partial decay widths Γ_f for the observed γ rays, and, subsequently, the level lifetime, τ, and reduced transition probabilities between the photo-excited level and the lower-lying final state. For none of the transitions connecting two positive parity levels is an $E2/M1$ multipole-mixing ratio, δ, known. Consequently, for all those transitions the two possible reduced transition probabilities $B(\Pi L)\downarrow$ are calculated and given as upper limits. For these limits, the calculated values are presented with the uncertainties given separately.

The inserts (a), (b), and (c) of Fig. 1 show peaks at 2964.7(9), 4280.0(8), and 6473.4(7) keV, which are identified as newly observed transitions from the 10712.3(5)-keV $J^\pi = 1^+$ level of ^{24}Mg. These transitions were assigned to this level using Ritz's variational principle and the known energies of the low-lying levels [3]. All other observed transitions associated with ^{24}Mg were previously known [3].

The observation of known transitions depopulating the 2^+ level at 10729 keV without observing the ground-state decay is rather unusual. However, the low-intensity peak corresponding to the ground-state decay is hidden in the high-energy tail of the 10712-keV peak, which dominates the recorded spectra. The reduced peak-to-background ratio does not allow for an identification of the peaks of the ground-state transition. Furthermore, since this branching ratio is also not given in the literature, no subsequent quantities can be deduced for the transitions depopulating this level. Nevertheless, in the future, once this branching ratio has been determined, the energy-integrated cross sections for the other transitions given in Table 3 will allow a calculation of quantities such as the decay width, level lifetime, and reduced transition probabilities.

In Table 4 the extracted level half-lives, $T_{1/2}$, are compared to those found in the literature, $T_{1/2,lit}$, [3]. Interestingly, while most extracted half-lives agree well with the adopted values [3], those for the 1^+ levels disagree. Those extracted in this work are approximately 30% longer than previously published values [7].

4 Discussion

In the literature [3,10], several $J^\pi = 1^-$ levels are known in ^{24}Mg. Since NRF is very sensitive to these levels, they should be excited if their $B(E1, 0^+ \rightarrow 1^-)$ strength is sizeable. However, only γ rays arising from the 1^- level at 8437 keV were statistically significant in the measured spectra. None of the γ-ray transitions from other known 1^- states were observed. In order to obtain at least an upper limit for the $B(E1)\uparrow$ strength, the sensitivity limit at the energy position of the ground-state decay and the ground-state branching ratio as found in the literature [3] were used to calculate an upper limit for the $B(E1)\uparrow$ strength. The corresponding data are given in Table 5.

Interestingly, this $N = Z$ nucleus does not exhibit noticable low-lying $E1$ strength. The upper limit is $B(E1)\uparrow \leq 0.61 \times 10^{-3}$ e^{2}fm^2. Of course, for the levels above the 9316.55-keV threshold for α-particle emission, possible depopulation via α-particle emission cannot be ruled out, es-

Table 2. The first two columns present the energy, E_i, and spin-parity combination, J_i^π, of the initial level, respectively. In column three the energy of the observed γ ray E_γ is given. Column four presents the spin and parity J_f^π of the final level. The spins and parities are taken from Ref. [3]. The measured ratio $W(90°)/W(127°)$ of the angular distributions at 90° and 127°, respectively, are also presented. If no $W(90°)/W(127°)$ ratio is given, the γ ray was only observed in the detectors positioned at 127°. The multipolarities of the transitions used in the calculation of the energy-integrated scattering cross section are also presented.

E_i [keV]	J_i^π	E_γ [keV]	J_f^π	$W(90°)/W(127°)$	$\Pi_1 L_1$-$\Pi_2 L_2$
1368.672(5)[a]	2^+	1368.626(5)[a]	0^+	1.13(8)	18.5 % $E2$-$E2$ + 81.5 % isotropic
4238.8(7)	2^+	4238.6(6)	0^+	1.41(14)	50 % $E2$-$E2$ + 50 % isotropic
		2870.3(8)	2^+	0.93(20)	50 % $E2$-$E2$ + 50 % isotropic
5235.0(10)	3^+	3866.3(10)	2^+	0.7(5)	isotropic
6432.3(7)	0^+	5063.6(7)	2^+	1.10(22)	isotropic
7348.2(7)	2^+	7348.5(9)	0^+	1.9(5)	$E2$-$E2$
		5979.3(8)	2^+	1.1(3)	isotropic
7747.5(12)	1^+	7748.1(21)	0^+		$M1$-$M1$
		6378.3(9)	2^+	1.0(4)	$M1$-$M1$
8437.2(9)	1^-	8438.7(9)	0^+	0.8(2)	$E1$-$E1$
		7067.1(14)	2^+	1.6(9)	$E1$-$E1$
9003.7(10)	2^+	9003.9(19)	0^+	2.8(20)	$E2$-$E2$
		7633.6(13)[b]	2^+	1.9(8)	$E2$-$E2$
		4882.3(17)	2^+	0.5(4)	$E2$-$M1$
9828.5(7)	1^+	9828.5(12)	0^+	0.73(8)	$M1$-$M1$
		8459.8(7)	2^+	0.87(12)	$M1$-$E2$
9967.7(7)	1^+	9967.8(12)	0^+	0.72(6)	$M1$-$M1$
		8599.0(7)	2^+	0.96(9)	$M1$-$M1$
10360.7(13)	2^+	10360.4(19)	0^+	2.4(17)	$E2$-$E2$
		8992.3(15)	2^+	1.2(5)	$E2$-$E2$
10712.3(5)	1^+	10711.5(11)	0^+	0.72(8)	$M1$-$M1$
		9343.6(12)	2^+	0.96(13)	$M1$-$M1$
		6473.4(7)	2^+	1.0(3)	$M1$-$M1$
		4280.0(8)	0^+	0.6(3)	$M1$-$M1$
		2964.7(9)	1^+	0.7(3)	$M1$-$M1$
10729.4(11)	2^+	9361.3(16)	2^+	0.6(3)	$E2$-$M1$
		6491.3(14)	2^+	0.8(7)	$E2$-$M1$
		5493.5(22)	3^+	0.6(6)	$E2$-$M1$

[a] Value from Ref. [3].
[b] Peak may be contaminated.

pecially when considering natural parity states. However, given the need for the α particle to tunnel through the ≈5.6 MeV high Coulomb barrier and that a photo-excited level must have a γ-ray decay channel, the non-observation of these γ rays indicates negligible $E1$ strength. Given the 11692.7 keV proton separation energy [3] and the positive parity of the $J^\pi = 3/2^+$ ^{23}Na ground state, the proton-emission channel can be excluded for the 1^- levels in Table 5. In the adjacent even-even nucleus ^{26}Mg a total of $\sum B(E1) \uparrow = 25(2) \times 10^{-3}$ e^{2}fm^2 [26] is observed. The ^{26}Mg(γ,γ') experiment was also conducted at the γELBE setup and used a similar end-point energy. Hence, the experimental sensitivity is practically identical. Consequently, experimental reasons can be ruled out

Table 3. The table presents the energy of the initial level, E_i, and its spin and parity, J_i^π, the γ-ray energy E_γ, the spin and parity, J_f^π, of the final level, the measured energy-integrated cross section, $I_{s,f}$, and the calculated reduced transition probabilities $B(M1)\downarrow$, $B(E2)\downarrow$, and $B(E1)\downarrow$. All spins and parities are taken from the NNDC database [3]. For levels that are clearly fed by higher-lying levels, $I_{s,f}$ is given only as an upper-limit. If for a parity-conserving transition no multipole-mixing ratio, δ, is known, both possible reduced transition probabilities are given as upper limits.

E_i [keV]	J_i^π	E_γ [keV]	J_f^π	$I_{s,f}$ [eV·b]	Γ_f [meV]	$B(M1)\downarrow$ [μ_N^2]	$B(E2)\downarrow$ [e^{2}fm^4][a]	$B(E1)\downarrow$ [10^{-6}e^{2}fm^2]
1368.672(5)[b,c]	2^+	1368.626(5)[b,c]	0^+	< 62	< 6.0		< 1480	
4238.8(7)[c]	2^+	4238.6(6)	0^+	< 7.7	< 9.6		< 9.4	
		2870.3(8)	2^+	< 2.3	< 2.9	< 0.00002[d]	< 19[d]	
5235.0(10)[e]	3^+	3866.3(10)	2^+					
6432.3(7)[e]	0^+	5063.6(7)	2^+					
7348.2(7)	2^+	7348.5(9)	0^+	3.9(6)	19(5)		1.1(3)	
		5979.3(8)	2^+	3.0(5)	15(4)	$\leq 0.006(2)$	$\leq 2.4(6)$	
7747.5(12)[c]	1^+	7748.1(21)	0^+	< 1.3	< 28	< 0.0054		
		6378.3(9)	2^+	< 3.2	< 84	< 0.027	< 10	
8437.2(9)	1^-	8438.7(9)	0^+	8.4(13)	61(20)			96(27)
		7067.1(14)	2^+	1.4(4)	10(4)			27(10)
9003.7(10)	2^+	9003.9(19)	0^+	2.8(9)	28(14)		0.6(3)	
		7633.6(13)[f]	2^+	2.7(6)	27(14)	$\leq 0.005(2)$	$\leq 1.3(5)$	
		4882.3(17)	2^+	1.1(3)	11(6)	$\leq 0.008(4)$	$\leq 5(2)$	
9828.5(7)	1^+	9828.5(12)	0^+	65(8)	730(130)	0.066(13)		
		8459.8(7)	2^+	22(3)	242(43)	$\leq 0.035(7)$	$\leq 7(2)$	
9967.7(7)	1^+	9967.8(12)	0^+	198(22)	2460(380)	0.214(37)		
		8599.0(7)	2^+	88(10)	1087(168)	$\leq 0.148(26)$	$\leq 29(6)$	
10360.7(13)	2^+	10360.4(19)	0^+	4.0(12)	68(25)		0.7(3)	
		8992.3(15)	2^+	8.2(16)	140(50)	$\leq 0.017(6)$	$\leq 3(1)$	
10712.3(5)	1^+	10711.5(11)	0^+	707(73)	8710(2880)	0.612(154)		
		9343.6(12)	2^+	141(16)	1734(574)	$\leq 0.184(47)$	$\leq 30(8)$	
		6473.4(7)	2^+	17(3)	211(70)	$\leq 0.067(18)$	$\leq 23(6)$	
		4280.0(8)	0^+	6.1(10)	75(25)	0.083(24)		
		2964.7(9)	1^+	4.5(9)	55(19)	$\leq 0.183(56)$	$\leq 0.299(91)$	
10729.4(11)	2^+	9361.3(16)	2^+	9.1(16)				
		6491.3(14)	2^+	2.3(8)				
		5493.5(22)	3^+	1.1(5)				

[a] 1 e^{2}fm^4 $\equiv$ 0.243 W.u.
[b] Value taken from Ref. [3].
[c] Level partially populated by feeding.
[d] Value calculated using multipol-mixing ratio from Ref. [3].
[e] Level exclusively populated by feeding.
[f] Peak in $\theta = 127^\circ$ spectrum possibly contaminated.

Table 4. Comparison of the level half-lives from this work, $T_{1/2}$, and the NNDC database values [3], $T_{1/2,lit}$. If only a lower-limit is given, this implies that the level was fed from higher-lying levels.

E_l [keV]	J_i^π	$T_{1/2}$ [fs]	$T_{1/2,lit}$ [fs]
1368.7	2^+	> 80	1360(30)
4238.7(8)	2^+	> 33	45.7(35)
7348.2(7)	2^+	13(3)	6.5(22)
7747.5(12)	1^+	$> 3.5^a$	12.5(28)
8437.2(9)	1^-	6(2)	9(2)
9003.7(10)	2^+	$6(3)^a$	8.4(12)
9828.5(7)	1^+	$0.46(9)^a$	0.30(7)
9967.7(7)	1^+	0.13(2)	0.071(7)
10360.7(13)	2^+	$2.1(6)^a$	1.0(3)
10712.3(5)	1^+	0.038(9)	0.023(2)
10729.4(11)	2^+		7(3)

[a] Calculated using additional transitions to lower-lying excited states recorded in Ref. [3] but not seen in this experiment.

Table 5. Given is the level energy, E_{1^-}, of known 1^- levels [3, 10], the ground-state branching ratio Γ_0/Γ as taken from the NNDC database [3], the upper limit for the energy-integrated scattering cross section $\leq I_{s,0}$ for the ground-state decay channel of the 1^- level and the upper-limit of $B(E1)\uparrow$ strength. The limits were estimated using the sensitivity limit at the expected peak position. For the definition of the used sensitivity limit see the text.

$E_{1^-}^a$ [keV]	Γ_0/Γ	$I_{s,0}$ [eV·b]	$B(E1)\uparrow$ [10^{-6}e^{2}fm^2]
7555.04(15)	0.47^a	≤ 0.8	≤ 56
8437.2(9)	0.88(9)	8.4(13)	288(81)
9145.99(15)	0.47^a	≤ 2.0	≤ 116
11389.8(11)	0.25^a	≤ 1.1	≤ 26
11864.9(13)	0.57^a	≤ 1.1	≤ 41

[a] Taken from literature [3,10].

Table 6. Given is the level energy, E_{level}, the spin and parity, J^π, of the excited level, the experimental branching ratio as defined in Eq. 6, and the K quantum number assigned using the values defined in Eq. 2.

E_{level} [keV]	J^π	$R_{al,exp}$	K
7747.5(12)	1^+	4.8(28)	(0)
8437.2(9)	1^-	0.28(13)	1
9828.5(7)	1^+	0.52(13)	1
9967.7(7)	1^+	0.69(15)	1
10712.3(5)	1^+	0.30(8)	1

and the increase of the $E1$ strength is clearly linked to the two additional neutrons and the dynamical division of the center-of-mass and the center-of-charge induced by them.

Interestingly, compared to Ref. [7] ($\sum B(M1)\uparrow = 3.9(5)\ \mu_N^2$), the $B(M1)$ excitation strength extracted in this work, $\sum B(M1)\uparrow = 2.7(5)\ \mu_N^2$, is reduced. However, no such trend is observed for ^{26}Mg (Ref. [7]: $\sum B(M1)\uparrow = 2.9(2)\ \mu_N^2$ and the work at γELBE [26]: $\sum B(M1)\uparrow = 2.9(2)\ \mu_N^2$). Remarkably, the results for ^{24}Mg and ^{26}Mg as published in Ref. [7] were obtained at two different facilities. Given that Ref. [7] does not provide any details about how the detector efficiencies and photon fluxes were determined, it is impossible to comment on these values. One source of systematic error in the present measurement might be the target material, which is hygroscopic. An eventual contamination of the target material with water would for the measured mass reduce the number of target nuclei and, consequently, the extracted scattering cross section would appear too low. However, the material was unsealed immediately prior to the weighting process. Despite these uncertainties, the $M1$ strength extracted from the present experiment is comparable with the results for ^{26}Mg. Given the similar shell structure, for the Gamow-Teller resonances, a comparable $M1$ strength can be expected.

In Table 6, the branching ratios calculated using Eq. 6 are presented for the $J = 1$ levels. For the 1^+ levels the assumption is made, that the decay to the 2_1^+ level is of pure $M1$ multipolarity. For the assigned 2^+ levels, the low intensity of the transitions originating from these levels renders such an analysis obsolete. The low-intensity and associated large uncertainty of the transitions from the 7747-keV level prevent a firm assignment of a K quantum number; however, the levels at 8437, 9829, and 9968 keV all exhibit branching ratios that are consistent with an assignment of $K = 1$ within two standard deviations. The value for the level at 10712 keV is three standard deviations off. Nevertheless, even when assuming an $E2$ contribution in the decay to the 2_1^+ level, the branching ratio clearly favours a $K = 1$ assignment. The proximity of ex-

perimental to theroretical branching ratios, as far as the values have uncertainties within a reasonable limit, can be seen as a strong indication for the validity of the Alaga rules and, therefore, the well-deformed nature of ^{24}Mg.

The following discussion concerning the mixing of the ground state and the first excited 0^+ level relies on the thoughts outlined in Ref. [17]. Given the shape coexistence of the prolate deformed ground state and the superdeformed structure built upon the first excited 0^+ level at 6432 keV [13], the enormous $\rho^2(E0)$ value [18] provides evidence for the mixing of these structures. Hence, in a naive two-state mixing model, the physically observed states $|0^+_{gs}\rangle$ and $|0^+_2\rangle$ can be written as linear combinations

$$|0^+_{gs}\rangle = \cos\alpha|0^+_{prol}\rangle + \sin\alpha|0^+_{SD}\rangle$$

$$|0^+_2\rangle = -\sin\alpha|0^+_{prol}\rangle + \cos\alpha|0^+_{SD}\rangle.$$

Here, α is the mixing angle and $\sin\alpha$ and $\cos\alpha$ are the mixing amplitudes. Assuming that the wavefunction of the 10712-keV $J = 1$ level is dominated by one-particle one-hole excitations built upon the structure of the ground state, the observed decay to the 6432-keV level corresponds to the decay to the prolate $|0^+_{prol}\rangle$ component mixed into this level. Hence, the ratio of the mixing amplitudes can be extracted from the experimental ratio R_0 of the $B(M1)$ transition strengths.

$$R_0 = \frac{B(M1, 1^+_i \rightarrow 0^+_2)}{B(M1, 1^+_i \rightarrow 0^+_{gs})} = \left[\frac{\sin\alpha}{\cos\alpha}\right]^2.$$

Again, as previously mentioned for the Alaga rules, in the determination of the $B(M1)$ strength, the total decay width, Γ, and, therefore, uncertainties associated with the other γ rays depopulating the level of interest enter. To circumvent these additional uncertainty, the ratio R_0 can be transformed to

$$R_0 = \frac{I_{S,0^+_2}}{I_{S,0^+_{gs}}} \cdot \frac{E^3_{\gamma,0^+_{gs}}}{E^3_{\gamma,0^+_2}} = 0.13^{+0.05}_{-0.03},$$

where the integrated scattering cross sections $I_{S,f}$ with smaller relative uncertainties enter. This approach results in mixing amplitudes of $\cos\alpha = 0.94^{+0.02}_{-0.02}$ and $\sin\alpha = 0.34^{+0.05}_{-0.04}$, which, when neglecting any form of triaxiality, enter the equation (see Eq. 45 in Ref. [13])

$$\rho^2(E0) = \left(\frac{3Z}{4\pi}\right)^2 \cos^2\alpha \cdot \sin^2\alpha \left(\beta^2_{2,prol} - \beta^2_{2,SD}\right)^2.$$

Here, Z is the proton number and $\beta_{2,prol}$ and $\beta_{2,SD}$ are the quadrupole deformation parameters of the prolate deformed ground state and the superdeformed structure, respectively. The extracted mixing amplitudes are remarkably close to $\cos\alpha = 0.96$ and $\sin\alpha = 0.28$ [18] extracted from a shift of the 0^+_{gs} relative to the expected position from the energy pattern defined by the 2^+_1, 4^+_1, and 6^+_1 levels. Using the experimental value $1000 \times \rho^2(E0) = 380(70)$ [18] and the amplitudes extracted from this work, the difference in $\beta^2_{2,i}$ is calculated as

$$|\left(\beta^2_{2,prol} - \beta^2_{2,SD}\right)| = 0.67^{+0.20}_{-0.14}.$$

Of course, triaxiality was neglected and consequently the extracted difference of the deformation parameters is overestimated. Nevertheless, using the value $\beta_{2,prol} = 0.497(2)$ [18,27] for the ground state, results in $\beta_{2,SD} = 0.96^{+0.30}_{-0.08}$ for the deformation parameter of the superdeformed band. Hence, the present work confirms the results of Ref. [18] from an independent approach.

5 Summary

The present ^{24}Mg(γ,γ') experiment revealed only a negligible amount of $E1$ strength. This result indicates a link of low-lying E1 strength and an excess of one species of nucleons. In comparison to a previous (γ,γ') experiment this work provides a ≈ 30 % reduced $M1$ strength. However, the present result is comparable to the $M1$ strength observed in ^{26}Mg. An application of the Alaga rules indicates that ^{24}Mg is indeed a deformed nucleus and, the combination of a branching ratio from this work and the $10^3 \times \rho^2(E0)$ value from Ref. [18] allowed a confirmation of the assignment of a superdeformed nature to the 0^+ level at 6432 keV.

6 Acknowledgment

The collaboration is indebted to the ELBE-Beschleuniger Mannschaft for the excellent electron beams delivered in difficult Covid-19 times. The members of the UWS Nuclear Physics Research Group acknowledge financial support from the UK Science and Technology Facilities Council (STFC, Grant No. ST/P005101/1). The TU Darmstadt members acknowledge financial support by the Deutsche Forschungsgemeinschaft (DFG, German Research Foundation) under Grant No. SFB 1245 (project ID 279384907). This material is based upon work supported by the U.S. Department of Energy, Office of Science, Office of Nuclear Physics, under Grants No. DE-FG02-97ER41041 (UNC), No. DE-FG02-97ER41033 (TUNL). This work was supported in part by the U. S. National Science Foundation Grant No. PHY-2209678. The University of Kentucky members acknowledge taht this work is based in part upon work supported by the US National Science Foundation under Grant No. PHY-2209178. PA gratefully acknowledges the support by the Claude Leon Foundation in form of a postdoctoral fellowship. MV acknowledges the Slovak Research Agency under Contract No. APVV-20-0532, Slovak grant agency VEGA (Contract No. 2/0067/21) and the Research and Development Operational Programme funded by the European Regional Development Fund, Project No. ITMS code 26210120023 (20%) and funding from the ESET Foundation (Slovakia).

References

1. I. J. Thompson and F. M. Nunes, *Nuclear Reactions for Astrophysics*, (Cambridge University Press, 2009)
2. S. G. Ryan and A. J. Norton, *Stellar Evolution and Nucleosynthesis*, (Cambridge University Press, 2010)
3. M. Shasuzzoha Basunia and A. Chakraborty, Nucl. Data. Sheets **186**, (2022) 2.
4. M. Shasuzzoha Basunia and A. Chakraborty, Nucl. Data. Sheets **171**, (2021) 1.
5. U. Kneissl, H. H. Pitz, and A. Zilges, Prog. Part. Nucl. Phys. **37**, (1996) 349.
6. A. Zilges, D. L. Balabanski, J. Isaak, and N. Pietralla, Prog. Part. Nucl. Phys. **122** (2022) 103903.
7. U. E. P. Berg, K. Ackermann, K. Bangert, C. Bläsing, W. Naatz, R. Stock, K. Wienhard, M. K. Brussel, T. E. Chapuran, and B. H. Wildenthal, Phys. Lett. B **140**, (1984) 191.
8. P. F. Bortignon, A. Bracco, and R. A. Broglia, *Giant Resonances*, (CRC Press, 1998).
9. M. Harakeh and A. van der Woude, *Giant Resonances* (Oxford University Press, Oxford, 2001).
10. P. Adsley, V. O. Nesterenko, M. Kimura, L. M. Donaldson, R. Neveling, J. W. Brümmer, D. G. Jenkins, N. Y. Kheswa, J. Kvasil, K. C. W. Li, D. J. Marin-Lambarri, Z. Mabika, P. Papka, L. Pellegri, V. Pesudo, B. Rebeiro, P. G. Reinhard, F. D. Smit, and W. Yahia-Cherif, Phys. Rev. C **105**, (2022) 024311.
11. D. Savran, T. Aumann, and A. Zilges, Prog. Part. Nucl. Phys. **70**, (2013), 210.
12. A. Bracco, E. G. Lanz, and A. Tamii, Prog. Part. Nucl. Phys. **106**, (2019), 360.
13. P. E. Garrett, M. Zielinska, and E. Clement, Prog. Part. Nucl. Phys. **124**, (2022), 103931.
14. G. Alaga, K. Alder, A. Bohr, and B. R. Mottelson, K. Dan. Vidensk. Selesk. Mat. Fys. Medd. **29**, (1955), 1.
15. D. Savran, S. Müller, A. Zilges, M. Babilon, M. W. Ahmed, J. H. Kelley, A. Tonchev, W. Tornow, H. R. Weller, N. Pietralla, J. Li, I. V. Pinayev, and Y. K. Wu, Phys. Rev. C **71**, (2005), 034305.
16. K. Heyde and J. L. Wood, Rev. Mod. Phys. **83**, (2011), 1467.
17. G. Rusev, R. Schwengner, F. Dönau, S. Frauendorf, L. Käubler, L. K. Kostov, S. Mallion, K. D. Schilling, A. Wagner, E. Grosse, H. von Garrel, U. Kneissl, C. Kohstall, M. Kreutz, H. H. Pitz, M. Scheck, F. Stedile, P. von Brentano, J. Jolie, A. Linnemann, N. Pietralla, and V. Werner, Phys. Rev. Lett. **95**, (2005), 062501.
18. J. T. H. Dowie, T. Kibedi, D. G. Jenkins, A. E. Stuchbery, A. Akber, H. A. Alshammari, N. Aoi, A. Avaa, L. J. Bignell, M. V. Chisapi, B. J. Coombes, T. K. Eriksen, M. S. M. Gerathy, T. J. Gray, T. H. Hoang, E. Ideguchi, P. Jones, M. Kumar Raju, G. J. Lane, B. P. McCormick, L. J. McKie, A. J. Mitchell, N. J. Spinks, and B. P. E. Tee, Phys. Lett. B **811**, (2020), 135855.
19. R. Schwengner, R. Beyer, F. Dönau, E. Grosse, A. Hartmann, A. R. Junghans, S. Mallion, G. Rusev, K. D. Schilling, W. Schulze, and A. Wagner, Nucl. Instrum. Methods A **555**, (2005), 211.
20. GEANT4 collaboration, Nucl. Instrum. Meth. A **506**, (2003) 250.
21. R. Moreh, W. C. Sellyey, and R. Vodhanel, Phys. Rev. C **22** (1980) 182; Erratum: Phys. Rev. C **23**, (1981) 2799.
22. G. Rusev, A. P. Tonchev, R. Schwengner, C. Sun, W. Tornow, and Y. K. Wu, Phys. Rev. C **79**, (2009) 047601.
23. J. H. Kelley and C. G. Sheu, Nucl. Phys. A **880**, (2012), 88.
24. M. J. Martin, Nucl. Data. Sheets **108**, (2007), 1583.
25. D. Gribble, C. Iliadis, R. V. F. Janssens, U. Friman-Gayer, Krishichayan, and S. Finch, Phys. Rev. C **106**, (2022) 014308.
26. R. Schwengner, A. Wagner, Y. Fujita, G. Rusev, M. Erhard, D. De Frenne, E. Grosse, A. R. Junghans, K. Kosev, and K. D. Schilling, Phys. Rev. C **79**, (2009) 037303.
27. S. Raman, C. W. Nestor Jr., P. Tikkanen, At. Data Nucl. Data Tables **78**, (2001) 1.